

**Galactic Indigestion:  
Numerical Simulations of the Milky Way's Closest Neighbor**

Rodrigo A. Ibata<sup>1,2</sup> & Geraint F. Lewis<sup>3,4</sup>

Received \_\_\_\_\_;    accepted \_\_\_\_\_

Submitted to the Astrophysical Journal

---

<sup>1</sup>Department of Physics and Astronomy, University of British Columbia  
2219 Main Mall, Vancouver, B.C., V6T 1Z4, Canada

<sup>2</sup>Present address: European Southern Observatory  
Karl Schwarzschild Straße 2, D-85748 Garching bei München, Germany  
Electronic mail: ribata@eso.org

<sup>3</sup>Department of Physics and Astronomy, University of Victoria  
PO Box 3055, Victoria, B.C. Canada V8W 3P7  
Electronic mail: gfl@uvastro.phys.uvic.ca

<sup>4</sup>Department of Astronomy, University of Washington  
Seattle, Washington, U.S.A.  
Electronic mail: gfl@astro.washington.edu

## ABSTRACT

Are dwarf spheroidal galaxies dark matter dominated? We present N-body simulations of the interaction between the Milky Way and its closest companion, the Sagittarius dwarf spheroidal galaxy, constrained by new kinematic, distance and surface density observations detailed in a companion paper. It is shown that there is no possible self-consistent solution to the present existence of the Sagittarius dwarf if its distribution of luminous matter traces the underlying distribution of mass. The luminous component of the dwarf galaxy must therefore be shielded within a small dark matter halo. Though at present we are unable to construct a fully self-consistent model that includes both the stellar and dark matter components, it is shown numerically that it is possible that a pure dark matter model, approximating the dark matter halo deduced for the Sagittarius dwarf from analytical arguments, may indeed survive the Galactic tides.

The orbit of the Sagittarius dwarf around the Milky Way is considered, taking into account the perturbative effects of the Magellanic Clouds. It is shown that at the present time, the orbital period must be short,  $\sim 0.7$  Gyr; the initial orbital period for a  $10^9 M_\odot$  model will have been  $\sim 1$  Gyr. It is found that a close encounter with the Magellanic Clouds may have occurred, though the chances of such an interaction affecting the orbit of the Sagittarius dwarf is negligible.

*Subject headings:* numerical simulations, dwarf spheroidal galaxies, dark matter, Magellanic Clouds

## 1. Introduction

The Sagittarius dwarf galaxy (Ibata, Gilmore & Irwin 1994, 1995), the closest satellite galaxy of the Milky Way, provides an ideal laboratory in which the complex interactions that take place during the merging of galaxies may be probed. Motivated by these considerations, much information has now been gained on its kinematics, metallicity and stellar populations; the observational constraints obtained hitherto are reviewed in Ibata *et al.* (1997; hereafter referred to as IWGIS).

A particularly interesting assertion that results from an analysis of these data is that the sheer existence of the Sagittarius dwarf at the present time is very surprising. Accurate kinematic and distance data, which now sample most of the extent of the Sagittarius dwarf spheroidal, imply (subject to an assumption scrutinized in section 3 below) that this dwarf galaxy has a short orbital period around the Milky Way, less than  $\sim 1$  Gyr. Previously published numerical experiments of the disruption of this dwarf galaxy (Velasquez & White, 1995; Johnston *et al.*, 1995) showed that it is unlikely to survive more than a few perigee passages. Taking the results of these simulations to their logical conclusion, IWGIS argued that the observed stellar population cannot trace the mass of that dwarf galaxy, as the Sagittarius dwarf spheroidal would have been destroyed by the Galactic tides long ago. A self-consistent solution to the present existence of the dwarf can then only be found if the requirement that light traces mass is relaxed. Using the simple Jacobi-Roche tidal disruption criterion, IWGIS proposed a solution in which the stellar component of the dwarf galaxy is enveloped in a halo of dark matter, which has a mass profile such that dark matter density at the photometric edge of the dwarf is sufficiently high to impede tidal disruption. To be consistent with the observed low velocity dispersion of the stellar component embedded therein, the core radius of the dark halo would have to extend out to the photometric edge of the system.

The dwarf spheroidal companions of the Milky Way have long been suspected to contain large quantities of dense dark matter (e.g., Faber & Lin 1983; Irwin & Hatzidimitriou 1995), so the above conclusion for the specific case of the Sagittarius dwarf is perhaps not surprising; however, the density profile of the dark matter deduced by IWGIS has important implications for the nature of the dark halos and their constituents. Most of the dwarf spheroidals contain stars with a broad range of ages and metallicities, which is unexpected in the simplest explanation for their low mean metallicities — that chemical evolution was truncated by supernovae-driven winds (e.g., Sandage 1965; Dekel & Silk 1986); this problem may be alleviated with the dark matter halo model proposed by IWGIS, due an enhancement of the escape velocity from the dwarf galaxy.

These considerations about the dark matter content of the Sagittarius dwarf have substantial implications for the currently-popular hierarchical clustering picture of structure formation, such as Cold-Dark-Matter dominated cosmologies. A very significant accretion and merging of smaller systems occurs during the evolution of a normal galaxy like the Milky Way; is this still an on-going process?

In this paper we aim to examine IWGIS’ claims, redoing their approximate analytical calculations with numerical disruption experiments. These simulations will be constrained with all available relevant data. In particular, we will first investigate whether the assumption adopted by IWGIS in determining the orbit of the Sagittarius dwarf holds true, and so establish the best-fit orbit; and secondly, we will attempt to find a self-consistent solution to the present existence of the dwarf galaxy. This provides the necessary detailed analysis to determine the validity of IWGIS’ assertion.

## 2. Simulations

The numerical N-body simulations presented below were performed using the `box_tree` tree code program (version 2.1), kindly provided by D. Richardson (Richardson 1993). In all simulations, the tree-code opening angle was set to  $\theta = 0.5$ , and quadrupole correction was used.

### 2.1. Galactic potential model

The forces of the Milky Way on the dwarf galaxy are calculated by including into the `box_tree` program one of two models for the Galactic potential. For the majority of the simulations, we use an analytic model, detailed in Johnston *et al.* (1995), which is composed of a sum of three rigid potentials, with the disk component described by a Miyamoto-Nagai (1975) model,

$$\Phi_{disk} = -\frac{GM_{disk}}{(R^2 + (a + \sqrt{z^2 + b^2})^2)^{1/2}}, \quad (1)$$

the combined halo and bulge by a spherical Hernquist potential (Hernquist 1990),

$$\Phi_{sphere} = -\frac{GM_{sphere}}{(r + c)}, \quad (2)$$

and the dark halo by a logarithmic potential,

$$\Phi_{halo} = v_{halo}^2 \log(r^2 + d^2). \quad (3)$$

In these expressions,  $R$  and  $z$  are in cylindrical coordinates, while  $r$  is the radial distance in spherical coordinates;  $M_{disk} = 1.0 \times 10^{11} M_{\odot}$ ,  $M_{sphere} = 3.4 \times 10^{10} M_{\odot}$ ,  $v_{halo} = 128$  km/s,  $a = 6.5$ ,  $b = 0.26$ ,  $c = 0.7$  and  $d = 12.0$ , all in kpc. This combination of parameters yields an almost flat rotation curve between 1 and 30 kpc.

Two of the simulations carried out below were performed with a potential derived from the Galactic mass model of Evans & Jijina (1994). In this model, the disk component,

described by a double exponential disk, has radial scale length  $h_R = 3.5$  kpc and a Solar neighborhood surface density of  $\Sigma_0 = 48 M_\odot/\text{pc}^2$ . We further assume that the vertical scale length of the disk is  $h_z = 0.25$  kpc, and that the density falls to zero at  $R = 5h_R$ . The potential corresponding to this density distribution is found by multipole expansion of the Poisson equation using an algorithm described in Englmaier (1997). The halo component is described by a ‘power-law’ halo, so the potential has the following analytical expression:

$$\Psi = \frac{v_0^2 R_c^\beta / \beta}{(R_c^2 + R^2 + z^2 q^{-2})^{\beta/2}}, \quad \beta \neq 0,$$

where  $R$  and  $z$  are Galactocentric cylindrical coordinates, the core radius  $R_c = 2$  kpc,  $v_0 = 138 \text{ km s}^{-1}$ , and the exponent  $\beta = -0.2$ . The parameter  $q$  sets the oblateness of the equipotential surfaces; two values of this parameter were probed,  $q = 1$  and  $q = 0.9$ , corresponding to, respectively, a spherical halo and a halo with mass-flattening of  $\sim 0.7$ .

## 2.2. Dynamical friction

As a massive object moves through the Galactic halo, the halo responds (in a way that is dependent on the density and kinematics of the halo, and the mass and velocity of the object) to the extra gravitational attraction, leaving a wake of halo material behind the object. This wake, in turn, exerts a force back on the object in the direction opposing its direction of motion, a phenomenon termed dynamical friction. The effect of dynamical friction on the galaxy models we consider is significant, but not overwhelming. This can be seen by considering the orbital decay time  $t_{fric}$  due to dynamical friction of a satellite galaxy; an explicit expression is given by Binney & Tremaine (1987) for the particular case of a satellite on a circular orbit in a potential of constant circular velocity. The mean Galactocentric distance (averaged over an orbit) of the Sagittarius dwarf is  $\gtrsim 25$  kpc, while the most massive models considered below have  $M \sim 10^9 M_\odot$ ; with these assumptions  $t_{fric} > 10$  Gyr, so that such a model could have reduced its initial mean orbital radius by at

most a factor of 2. Since  $t_{fric} \propto M^{-1}$ , models with  $M \sim 10^8 M_\odot$  will hardly be affected at all.

The best way to account for this frictional force is to include a “live” halo of particles in the simulation. However, the implementation of this solution is not straightforward. First, for the halo to respond to the passage of the dwarf, sufficient spatial resolution is needed. If we require that there be at least  $\sim 100$  halo particles in the volume occupied by the dwarf at any point in its orbit, and take that  $\rho_{halo}(r) \propto r^{-2}$  (between the peri- and apoGalactic distances of 15 and 60 kpc), then  $> 3 \times 10^6$  particles are needed to model the halo (significantly more if one chose to populate the Galactic halo with particles interior to 15 kpc). Second, the distribution function of the Galactic halo is currently unknown, so a range of halo models would have to be explored. The computational power required for these calculations is well beyond that presently available to the authors.

So to make this problem tractable, we take advantage of an analytical approximation; dynamical friction is included into the `box_tree` program by means of an additional external force on each of the simulation particles, calculated as follows. First, we assume that only the Galactic dark halo contributes any significant friction to the simulation particles (which is reasonable given the peri-Galactic distance of the dwarf), that the velocity distribution in the dark halo is a Maxwellian distribution of dispersion  $\sigma$  (of value  $220 \text{ km s}^{-1}$ , set to be approximately equal to the circular velocity of the halo), and that the dark matter particles that make up the Galactic dark halo are of much lower mass than the simulation particles (which typically have masses  $> 10^4 M_\odot$ ). These assumptions simplify the Chandrasekhar dynamical friction formula to the following relation (Binney & Tremaine 1987):

$$\frac{d\vec{v}_i}{dt} = -\frac{4\pi \ln \Lambda G^2 \rho M_a}{\bar{v}^3} \left[ \text{erf}(X) - \frac{2X}{\sqrt{\pi}} e^{-X^2} \right] \vec{v} \quad (4)$$

where  $\vec{v}$  is the mean velocity of particles within a radius of  $R_a$  of the  $i$ th simulation particle,  $M_a$  is the total mass of particles within the same radius, and  $X \equiv \bar{v}/(\sqrt{2}\sigma)$ . In

all of the simulations of the internal structure of the Sagittarius dwarf, we set  $R_a = 5$  kpc, which is substantially larger than the radius of bound particles in all models. This choice of  $R_a$  has the effect of essentially eliminating dynamical friction on particles outside the bound clumps. The term  $\ln \Lambda$  is the Coulomb logarithm, defined such that  $\Lambda \equiv b_{\max} V_0^2 / G(M_a + m)$ , where  $b_{\max}$  is the largest impact parameter between the clump of mass  $M_a$  and initial velocity  $V_0$ , and a galaxy with constituent particles of mass  $m$ . Given that  $M_a \gg m$ , it follows that  $\Lambda \sim b_{\max} \bar{v}^2 / GM_a$ . Adopting  $b_{\max} = 100$  kpc (an approximate upper limit to the size of the Milky Way halo) the Coulomb logarithm (calculated for individual particles) takes on values in the (quite narrow) range  $8 \lesssim \ln \Lambda \lesssim 12$  for the (rather large) range of models considered below. Clearly  $\ln \Lambda$  is quite insensitive to the guessed value of  $b_{\max}$  adopted above.

There is a concern that the Chandrasekhar relation overestimates the dynamical friction, as phase mixing in the halo tends to dilute the wake behind the satellite. However, this does not pose a problem to our study, since we are primarily interested in placing lower limits on the survival time of the Sagittarius dwarf. The effect of overestimating the frictional force is to increase the lifetime of the dwarf galaxy, as the dwarf has to be placed on an initially longer period orbit (hence less disruption) than would be required in the absence of dynamical friction.

### 3. Search for a self-consistent model: can light trace the mass?

Our analysis is motivated by the claim that the Sagittarius dwarf spheroidal cannot have survived until the present day if its light traces its mass given its observed extent and velocity dispersion, and assuming that the orbit calculated by IWGIS is correct. This last assumption needs to be discussed in detail. IWGIS fitted the orbit of the Sagittarius dwarf spheroidal, by considering the orbit of its center of mass and comparing the distance and



projected line of sight velocity along the locus of the orbit to mean distance and mean radial velocity measurements along the major axis of the Sagittarius dwarf. Successive refinements to the initial three-dimensional velocity of the center of mass allowed iteration to a best-fitting solution. However, this calculation requires two assumptions. First, that the observed direction of elongation of the dwarf galaxy is closely aligned with its motion vector. Numerical simulations show that the tidal debris is confined to the orbital plane of the progenitor (Oh *et al.* 1995, Piatek & Prior 1995, Johnston *et al.* 1995, Velasquez & White 1995). Since the Sagittarius dwarf is seen behind the Galactic center, our line of sight must be almost in the orbital plane, so the observed projected elongation should indeed be aligned with its proper motion vector to very good approximation. The second assumption is that, for the purpose of the orbit calculation, the Sagittarius dwarf can be modeled as a collection of massless particles. This proposition is less clearly true; IWGIS argued that it is a fair approximation, but could not show it.

In the remainder of this section, we will consider carefully a grid of models that cover the plausible parameter space of proto-dwarf galaxy structure. We are aiming to answer definitively the question of whether any combination of initial structural and kinematic parameters can guarantee the survival of the Sagittarius dwarf until the present day, while yielding a present-day structure that is a good representation of the observations. We first list the constraints that determine the allowable orbits, the initial distribution function, and the allowable evolution of our models.

The following parameters determine the orbit:

- (i) The distance to the center of mass is  $25 \pm 1$  kpc (Ibata *et al.* 1994, Mateo 1995).
- (ii) The radial velocity of the center of mass in a non-rotating reference frame centered at the present position of the Sun is  $171 \pm 1$  km s<sup>-1</sup> (IWGIS).

(iii) As discussed above, the proper motion vector of the Sagittarius dwarf must be aligned parallel to the Galactic coordinate line  $l = 5^\circ$  (Ibata *et al.* 1994, IWGIS). This puts it on essentially a polar orbit. The component of the proper motion of the central regions of the Sagittarius dwarf in the direction perpendicular to the Galactic plane has been measured (Irwin *et al.* 1996, IWGIS), indicating that it is moving northwards with a transverse velocity of  $250 \pm 90 \text{ km s}^{-1}$ .

The following parameters determine the initial distribution function:

(iv) A firm lower bound to the present total mass is  $10^7 M_\odot$ , an estimate based on starcounts of red giant members (Ibata *et al.* 1994). In particular, that early work covered only a small fraction of the extent of the galaxy near its photometric center. (Note that the most massive globular cluster of the Sagittarius dwarf system, M54, alone has a mass of  $2 \times 10^6 M_\odot$  — Pryor & Meylan 1993). However, a lower limit of  $\sim 10^8 M_\odot$  is obtained from comparison of its mean metallicity to trends observed in the dwarf galaxy population (Ibata *et al.* 1995); since this last estimate better reflects the *initial* total mass (rather than the total mass after significant dynamical evolution in the tidal field of the Milky Way), we adopt  $\sim 10^8 M_\odot$  as the lower limit of the initial mass of the models.

(v) The present concentration of the stellar population in the Sagittarius dwarf is  $c \sim 0.5$  (IWGIS). The initial stellar concentration, is of course unknown, but may be estimated by comparison to other ellipsoidal galaxies. Of the Milky Way dSphs, the most concentrated is Sculptor, with  $c = 1.12$  (Irwin & Hatzidimitriou 1995). As a firm upper limit we adopt a maximum initial concentration of  $c = 2.1$  in our models. (The value  $c = 2.1$  corresponds to a central value of  $(\Psi/\sigma^2)_0 = 9$  in the formalism of Binney & Tremaine 1987, which we follow below, where  $\Psi$  is the relative potential and  $\sigma$  is a model parameter related, but not equivalent, to the central velocity dispersion). This choice is conservative, since only dynamically very evolved stellar systems have significantly higher concentration.

(vi) It was observed that the models never evolved to a state with a higher central velocity dispersion; we therefore investigated models with velocity dispersion equal to, or higher than the observed present velocity dispersion of the dwarf.

While the conditions that determine acceptable evolution are:

(vii) At the end of the integration, required to be the present day, the center of mass of the model must be located at the observed position of the center of the Sagittarius dwarf:  $R = 25 \pm 1$  kpc, ( $\ell = 5^\circ, b = -14.5^\circ$ ). The dispersion of radial velocities at the center of the model must be consistent with the observed value,  $\sigma_v = 11.4 \pm 0.7$  km s<sup>-1</sup> (IWGIS). The projected velocity and distance gradients must also match the observations.

(viii) The final minor axis half-mass radius must match the observed minor axis half-brightness radius  $R_{HB} \sim 0.55$  kpc (IWGIS).<sup>5</sup>

(ix) The Sagittarius dwarf spheroidal cannot have lost most of its luminous mass. It contains four globular clusters and a substantial stellar component concentrated over a region less than  $30^\circ$  in length. For instance if the Sagittarius dwarf, as observed at the present time, had only 25% of its original mass within the observed extent (i.e., within 5 kpc of the photometric center), the remaining 75% — in this case  $\sim 16$  globular clusters and a substantial stellar population — would be visible as a dense ring of globular clusters and tidally disrupted debris around the Milky Way. This, however, is not observed. We therefore stipulate that, at the end point of the integration, an acceptable model should retain 25% of the initial mass within 5 kpc of the photometric center.

(x) The Sagittarius dwarf spheroidal must retain a central concentration for at least

---

<sup>5</sup>The half-brightness radius was determined from the distribution of red clump stars in the Sagittarius dwarf. In the absence of a dark matter component,  $R_{HB}$  will be equal to the half-mass radius only if there has been no significant mass segregation.

12 Gyr (the age of its dominant stellar population Fahlman *et al.* 1996).

To start the N-body simulations, a suitable initial position and velocity for the center of mass of the model must be found. To this end, a point-mass particle is first integrated back in time for 12 Gyr in the chosen Galactic potential. The information needed for this calculation is: the present 3-D position of the center of mass, its radial velocity, and the projected direction of the velocity vector of the center of mass, all of which are accurately known; plus the proper motion, which is poorly constrained. Specific to each model, to calculate the orbital decay due to dynamical friction, one also requires the model mass, and the mass loss rate due to the tidal disruption. Since the mass loss rate is not known before the simulation has been completed, we assume that no mass loss occurs; this strategy increases the survivability of the models (since the model has an initially longer orbit), consistent with our aim of placing a lower limit on the survival time of the Sagittarius dwarf. The large inaccuracy of the proper motion measurement means that the magnitude of the present velocity of center of mass of the dwarf,  $|v_{com}|$ , is poorly constrained; to circumvent this problem we consider four orbits with  $|v_{com}| = 332 \text{ km s}^{-1}, 362 \text{ km s}^{-1}, 392 \text{ km s}^{-1}$  and  $422 \text{ km s}^{-1}$ , which we label ‘a’, ‘b’, ‘c’ and ‘d’ respectively. Orbit ‘a’ is the best-fit orbit found by IWGIS. It is uninteresting to simulate models where  $|v_{com}| < 332 \text{ km s}^{-1}$ , as this leads to shorter periods than that of orbit ‘a’ which simply aggravate the survivability problem. The  $R$ - $z$  structures of these orbits calculated for a test particle of negligible mass (i.e., no dynamical friction) are shown in Figure 1, where we have integrated the orbits back in time for 12 Gyr under the influence of the fixed Galactic potential described in Johnston *et al.* (1995).

The initial configuration of positions and velocities is constructed by choosing particles randomly from a King model (King 1966). King models fit the surface brightness of dSph quite acceptably (e.g., Irwin & Hatzidimitriou 1995), and are therefore a reasonable choice

for the distribution function of the protogalaxy. Three parameters are required to describe the model: following Binney & Tremaine (1987), these are the ratio of the central value of the relative potential  $\Psi$  to the square of the  $\sigma$  parameter, i.e.,  $(\Psi/\sigma^2)_0$ , the parameter  $\sigma$ , and the central value of the mass density  $\rho_0$ .

The starting parameters of the King models are given in Table 1. The columns of this table list: (1) the model identification label, where the letter following the hyphen gives the orbit label; (2) the value of  $(\Psi/\sigma^2)_0$ ; (3) the central mass density,  $\rho_0$ ; (4) the  $\sigma$  parameter of the model; (5) the one-dimensional velocity dispersion of the model,  $\sqrt{v_x^2}$ ; (6) the half-brightness radius,  $R_{HB}$ ; (7) the tidal radius,  $R_T$ ; (8) the total mass of the model,  $M$ ; and (9) the number  $N$  of equal mass particles in the simulation.

Each structural model (listed in Table 1) was evolved in simulations of either 4000 or 8000 particles. To a reader familiar with the present state of numerical experiments in cosmology, simulations of a few thousand particles may appear ridiculously inadequate. However, the time-step choosing routine in Richardson’s (1993) code, adapts to the very short crossing time of particles the in the dwarf galaxy, and to changing forces on the dwarf due to the external potential, which vary on a short timescale due to its rapid orbital velocity. The limitation of 8000 particles, matching previous work (Johnston *et al.* 1995, Velasquez & White 1995, Piatek & Pryor 1995), was chosen because a single such simulation requires approximately one month of Sparc Ultra II cpu time to complete.

A significant concern with N-body simulations is that the behavior of the modeled system may not reflect the true dynamics, since due to the present computational limitations, each simulation particle usually represents many stars (or dark matter particles). Thus in the simulations, violent interactions of close particles are more destructive than in reality, while the diffusion of particles up to the escape velocity of the system, known as “evaporation”, leads to faster dissolution. The effect of close encounters in the simulations

may be reduced by artificially softening gravity forces; we chose a smoothing length of 100 pc, matching the simulations of Velasquez & White (1995). However, the effect of evaporation, being a result of long-range interactions, cannot be avoided. The evaporation time,  $T_{ev}$ , of a King model is typically between 1% and 6% of the half-mass relaxation time,  $T_{rh}$  (Johnstone 1993). With equal mass particles, we find (Spitzer 1987):

$$T_{rh} = \left(\frac{2}{3}\right)^{1/2} \frac{(\overline{v^2})^{3/2} N}{(M^2/2V_h)4\pi G^2 \ln \Lambda},$$

where  $\overline{v^2}$  is the mean-square velocity of the particles,  $N$  is the number of simulated particles,  $M$  is the mass of the model,  $V_h$  is its half-mass volume, and  $\ln \Lambda$  is the Coulomb logarithm. The evaporation timescale of our models (listed in column 10 of Table 1, using Figure 2 of Johnstone 1993 to relate  $T_{ev}/T_{rh}$  as a function of concentration) is longer than the 12 Gyr integration time of the simulations, except in the case of some concentrated models with high central density (K11 – K15). Evaporation effects are therefore likely to be significant for the models K11 to K15, so for these models the quoted survival times are lower limits.

For comparison of the disruption rates between models, we define two timescales: the time of “complete disruption”,  $T_{dis}$ , defined to be that time at which 90% of the simulation particles lie outside the Roche radius; and  $T_{ok}$ , the time at which the model becomes too unbound to be consistent with observations, which we set (for reasons mentioned above) to be the time at which more than 25% of the initial mass lies further than 5 kpc from the central concentration. The Roche radius of the system is calculated by determining the radius at which the mean density of the simulation particles becomes less than twice the Galactic mean density interior to the previous periGalactic distance of the orbit (recall that the periGalactic distance decays due to dynamical friction). Clearly, these calculations require the center of the model to be known. To this end, at every output timestep, we find the simulation particle from which the rms deviation to its nearest 100 neighbors is smallest, and choose this particle to represent the center of the dwarf galaxy (or dwarf

galaxy fragment). In Table 1, the quantities  $T_{dis}$  and  $T_{ok}$  are listed, respectively, in columns (11) and (12); however, when  $T_{dis}$  or  $T_{ok}$  exceed 12 Gyr, the same entries list, respectively, the fraction (in percent) of particles within the Roche radius, and the fraction of particles within 5 kpc of the center of the model.

To compare the velocity dispersion of the simulated models to observations, we calculate the radial velocity dispersion of particles within a projected radius of  $3^\circ$  from the center of the models, at the simulation time  $T_{ok}$ , as seen from the position of the Sun. This quantity,  $(\sqrt{v_r^2})_{T_{ok}}$ , is listed in column (13) of Table 1. Finally, the minor axis half-brightness radius, calculated at the simulation time  $T_{ok}$ , from particles in a 100 pc strip across the minor axis of the model, is listed in column (14).

### 3.1. The King model simulations

We started our simulations with the model K1-a, whose initial configuration fits best the observations of the present state of the Sagittarius dwarf. In particular, the one dimensional velocity dispersion  $(\overline{v_x^2})^{1/2}$  was set close to the observed value of  $11.4 \text{ km s}^{-1}$ , the minor axis half-mass radius was set close to the observed value of 0.55 kpc, and the model was placed on the best-fit orbit found by IWGIS (i.e., similar to the orbit of Figure 1a). The model disrupted rapidly, however; with complete disruption occurring after only 5.3 Gyr. These models confirm, using constraints from a more complete data set, the findings of Velasquez & White (1995) and Johnston *et al.* (1995) that models of the Sagittarius dwarf, in which light traces mass, are fragile. If so, one may deduce that the Sagittarius dwarf will be completely disrupted within  $\sim 5$  Gyr, providing a source of new stars and globular clusters to the Galactic halo. At the end of the integration, at 12 Gyr, the structure of the galaxy remnant is shown in Figure 2. No bound concentration of particles remains; instead, streams of particles populate the orbital path of the former dwarf galaxy.

As detailed above, the orbit presented by IWGIS was calculated using massless particles to trace the motion of the Sagittarius dwarf. Under that assumption, they found that the observed radial velocity gradient implied a short period orbit like that shown in Figure 1a. However, it is worth checking whether the internal self-gravity of the dwarf galaxy could act to accelerate stars along the tidally distorted major axis in a way that would mimic the velocity gradient of a shorter period orbit. We therefore performed further simulations (K1-b, K1-c, K1-d), where the model was placed progressively longer period orbits similar to those shown in Figure 1 on panels ‘b’, ‘c’ and ‘d’, respectively. The model K1-b disrupted completely before the end of the integration, while the models K1-c and K1-d retained an intact core (see Figures 3 and 4 and Table 1). However, the major axis velocity gradient at the end-point of K1-c and K1-d is much larger than that allowed by the observations, as we show in Figure 5. Furthermore, the velocity dispersion at the simulation end-point is too low, inconsistent with the observations.

The initial structure of the K1 models gives a good representation of the present state of the Sagittarius dwarf. Since these fail to survive in the Galactic potential, one can immediately deduce that either there has been significant structural evolution from the initial state, or that light does not trace mass in the Sagittarius dwarf. In the remainder of this section we explore the first of these options, delaying discussion of the second option to section 4.

The King models K1 – K8 were simulated to investigate the plausible range of initial models with fixed  $(\Psi/\sigma^2)_0 = 2.0$  (equivalent to an observed concentration  $c \sim 0.7$ ) which are consistent with the setup constraints listed above. The central density is increased from K1 to K8. Higher central density leads to smaller half-mass and tidal radii, which should yield more robust models. Indeed, the sequence of models K1, K3 and K5, which were set up to have initial velocity dispersion equal to the observed present velocity dispersion of



the dwarf, are a sequence of increasing robustness. The model K5-a is sufficiently robust to be consistent with the survival constraint, it has a radial velocity gradient also in good agreement with observations; however, its final central velocity dispersion,  $\sigma_v = 9.4 \text{ km s}^{-1}$ , is approximately 3 standard deviations lower than the observed value of  $11.4 \pm 0.7 \text{ km s}^{-1}$ .

Since the central velocity dispersion of our models was found to always decay as the disruption proceeds, we also simulated the K2, K4, K6, K7 and K8 models, where the initial value of the velocity dispersion was set substantially higher than the observed present day value. The K2 and K4 models, like their lower velocity dispersion counterparts K1 and K3, disrupted rapidly. Similarly, the very high velocity dispersion model K7 was also quickly destroyed by the Galactic tides.

However, the K6-a and K8-a models match the velocity dispersion and radial velocity observations quite well, and satisfy the survival time constraint. Contour maps of these models at the end point of the simulation, are shown in Figure 6. The axis ratios of the remnants are in good agreement with the deduced 3:1:1 ratio (IWGIS). However, the final minor axis half-brightness radii of both these models is  $R_{HB} = 0.15 \text{ kpc}$ , inconsistent with the observed value of  $R_{HB} \sim 0.55 \text{ kpc}$ .

More concentrated models may survive longer if their inner regions manage to stay stable while diffuse outer layers are lost to Galactic tides. This notion led us to undertake simulations with the models K9 – K15, whose concentration  $c = 1.25$  ( $(\Psi/\sigma^2)_0 = 6.0$ ) is slightly higher than that of the Sculptor dSph (the most centrally concentrated of the Galactic dSph), which has  $c = 1.12$  (Irwin & Hatzidimitriou 1995). From K9 to K16 we increase the central density while varying the velocity dispersion, thereby sampling a large range of plausible models at this concentration. It was found that models on the ‘b’, ‘c’ and ‘d’ orbits always have projected major axis kinematics that are inconsistent with observations. Surprisingly, the model K13-a survives the interaction with the Milky Way

almost completely intact, despite its relatively short evaporation timescale; this suggests that the method of Johnstone (1993) overestimates the evaporation rate in some situations.

Of the models with  $(\Psi/\sigma^2)_0 = 6.0$ , K10-a managed to survive the Galactic tides, and give a good representation of the kinematic observations. Again, however, the final minor axis half-brightness radius is  $R_{HB} = 0.14$  kpc, inconsistent with the observed value.

To check the survivability of less concentrated models we ran models K16 – K20. As found above, only those models on the ‘a’ orbit are able to reproduce the observed radial velocity gradient. Of these models, K17-a is sufficiently robust and gives a good representation of the observed kinematics. Yet its final half-brightness radius,  $R_{HB} = 0.17$  kpc, is again inconsistent with the observed value.

### 3.2. The effect of initial major axis rotation

Could the Sagittarius dwarf be a tumbling body, rotating along its major axis, so that the observed elongation is a consequence of rotation? This seems unlikely, as observations of dwarf ellipticals, in particular, NGC 147, NGC 185 and NGC 205 (Bender & Nieto 1990), show that they are not rotationally flattened. Nevertheless, could tumbling either imply a longer period orbit or lead to less disruption? IWGIS showed that clockwise linear rotation in the sense of Figure 1 implies a shorter orbital period, while longer periods are deduced for anti-clockwise rotation. By comparison to the ellipsoidal stellar models of Binney (1978), they argued that given the observed axis ratios (3:1:1), the maximum rotational velocity is likely to be at most equal to the velocity dispersion, i.e.,  $\sim 11 \text{ km s}^{-1}$ . Taking the then outermost major axis field (at  $b = -24.5^\circ$ ) as the major axis limit of the system, they deduced orbital periods of  $\sim 0.6$  Gyr and  $\sim 1.6$  Gyr for, respectively, clockwise and anti-clockwise linear rotation of the major axis around the center of mass. Since clockwise

rotation leads to shorter orbital periods and so to shorter survival times, only anti-clockwise rotation need be considered here.

It is interesting to note a general result valid for all of the spherical, initially non-rotating, models we investigated. As the dwarf becomes affected by the Galactic tides, its shape becomes elongated such that its leading edge is closer to the Galactic center than its trailing edge. The resulting force gradient torques the now slightly bar-like dwarf, which progressively gains spin angular momentum (presumably at the expense of a small amount of orbital angular momentum), until its outer stars become centrifugally unbound. The sense of the spin provided by the Galaxy to the dwarf is always the same as the sense of the orbit of the dwarf around the Galaxy. Placed on the same orbit, it transpired that models which have initial rotation in the same sense as their orbit dissolve faster than models whose initial rotation is in the opposing sense, apparently due to a cooperation with the Galaxy in the centrifugal expulsion of the outer particles. Since the proper motion measurement indicates that the orbit of the Sagittarius dwarf is anti-clockwise in the sense of Figure 1, anti-clockwise major axis rotation is expected to promote disruption.

The bar-like distortion induced by the tides near periGalacticon to the non-rotating models does not significantly affect the symmetry of their central regions (say defined as that region whose radius contains half the mass interior to the Roche limit), which remain approximately spherical until just before complete disruption. Thus the structure of initially non-rotating models is very different to that of models that have a significant fraction of their kinematic energy in rotation; in isolation the latter become prolate triaxial bars (see e.g., Binney & Tremaine 1987). On orbiting around the Galaxy, a prolate bar with a major axis rotation vector parallel to the rotation vector of its orbit will periodically point its major axis directly at the Galactic center. With the above axis ratios (3:1:1), the dominant tidal force along the line connecting the center of the Milky Way and the Sagittarius dwarf

will be periodically approximately 3 times larger than in a similarly-shaped non-rotating model (the latter, as discussed above, align themselves approximately along the orbit). Thus tumbling will lead to greater tidal disruption, worsening the survivability problem.

### 3.3. Summary: Constant $M/L$ models

In conclusion, we have attempted to model the interaction of the Sagittarius dwarf with the Milky Way under the assumption that the observed population of red clump stars traces the underlying mass distribution. With a few exceptions, these models had  $M/L \lesssim 10$ .

All the models placed initially on the ‘a’ orbit give rise to a radial velocity gradient that is in good agreement with the observations, while those models on the longer period ‘b’, ‘c’ and ‘d’ orbits give progressively worse fits to the radial velocity data. This gives a strong indication that the true orbit of the Sagittarius dwarf is close to the ‘a’ orbit, which has a short period  $T \lesssim 1$  Gyr, and implies that there have been many collisions with the Galactic disk in the past.

A thorough search of parameter space with a grid of 20 models has revealed several models (K5-a, K6-a, K8-a, K10-a, K13-a and K17-a) that retain a bound core at the end of the simulation, and fit the radial velocity profile. Of these, models K6-a, K8-a, K10-a and K17-a also fit the observed radial velocity dispersion. However, no model manages to survive and be consistent with the observed minor axis width of the Sagittarius dwarf: all models that have initially large half mass radii are rapidly destroyed by the Galactic tides.

In all the models, the half mass radius becomes smaller as disruption proceeds. So large initial half mass radii are required to match the final  $R_{HB} = 550$  pc. Yet any such model is rapidly destroyed by the Galactic tides.

It must be concluded that at least one of the assumptions laid out above is not valid.

IWGIS argued that the most plausible explanation for this quandary is that the visible component of the Sagittarius dwarf resides within a halo of dark matter which protects it against Galactic tidal forces. We further explore this claim below.

#### 4. A heavy course of dark matter

Having shown that models with constant  $M/L$  are unacceptable, we next investigate the survivability of models with dark matter halos.

IWGIS used the analytical Jacobi-Roche criterion to show that it is plausible that the stellar component of the Sagittarius dwarf could easily resist Galactic tides if it was embedded in a dark matter halo. For simplicity, the model presented was a homogeneous sphere of density  $\rho = 0.03 M_{\odot}/\text{pc}^3$ , which extended out to a cutoff at the visible minor axis limit of the system,  $r_c = 1.5 \text{ kpc}$ . Binney & Tremaine (1987) discuss the derivation of distribution functions for spherical systems from their density profile. They show that the distribution function of a spherical stellar system of density  $\rho(r)$  is given by:

$$f(\varepsilon) = \frac{1}{\sqrt{8\pi^2}} \frac{d}{d\varepsilon} \int_0^\varepsilon \frac{d\rho}{d\Psi} \frac{d\Psi}{\sqrt{\varepsilon - \Psi}}, \quad (5)$$

where  $\varepsilon$  and  $\Psi$  are respectively the relative energy and relative potential, and that the distribution function derived in this way is physical if and only if the expression

$$\int_0^\varepsilon \frac{d\rho}{d\Psi} \frac{d\Psi}{\sqrt{\varepsilon - \Psi}}, \quad (6)$$

is an increasing function of  $\varepsilon$ . Given that the potential of the homogeneous sphere is  $\Phi(r) = -2\pi G\rho(a^2 - \frac{1}{3}r^2)$ , it is clear that this model does not satisfy the above condition, so the homogeneous sphere cannot be a steady-state configuration for a collisionless self-gravitating system, as is intuitively obvious.

We were unable to solve equation 5 analytically to find the least concentrated collisionless self-gravitating spherical system that fulfills the condition of

equation 6; however, by trial and error we discovered that the following, almost homogeneous, density profile does give a physical distribution function (the profile is simply the central regions of a Gaussian):

$$\rho(r) = \rho_0 \frac{e^{-(rr_s/r_l)^2} - e^{-r_s^2}}{1 - e^{-r_s^2}}. \quad (7)$$

Here  $\rho_0$  is the central density,  $r_s$  is a scale radius, and  $r_l$  is the limiting radius of the system. In Figure 7, this profile (for  $r_s/r_l = 1$ ) is compared to our very low concentration King model K17.

Ideally, we would have modeled both the dark matter and stellar components as collisionless dynamical systems and simulated both with the N-body code. One would then have been able to compare the modeled stellar component to the observed kinematics and observed light profile. However, this is a very difficult numerical task, as, in order to avoid mass segregation, all the particles in the simulations must have the same mass. Since the mass to light ratio of the Sagittarius dwarf deduced by IWGIS is  $M/L \sim 100$ , the number of particles in the combined stellar and dark matter simulation would have to be  $\sim 10^6$  in order to obtain a useful resolution in the stellar component. So in the present contribution, we only consider the dark matter, which must be the principal contributor to the potential, if it is to solve the problem of the survival of this dwarf galaxy.

We experimented releasing models on the ‘a’ orbit with a range of structural parameters into the fixed Milky Way potential. It is uninteresting to describe these pure dark matter models at any length, since there is relatively little to learn from their end-point structure given that these cannot be compared to observations. We were contented to find that one such model, of  $N = 8000$  particles, and with parameters  $M = 1.2 \times 10^9 M_\odot$ ,  $r_s = 1$  kpc,  $r_l = 1$  kpc, managed to survive largely intact at the end of the simulation (42% of the particles remained inside  $T_{ok}$ ). Contrary to what was found in the simulation of the King models, the present-day minor axis half-mass radius for this dark matter model,

$R_{HB} = 0.7$  kpc, is more extended than the stellar component.

Thus one can construct dark matter models that survive the Galactic tides. The last example gives a flat, extended dark matter profile, as required by the analytical dark matter halo model proposed by IWGIS. However, given the absence of a luminous component in the simulations, at the present time we are unable to make a useful comparison to observations.

## 5. Discussion

### 5.1. The assumptions

#### 5.1.1. *The choice of Galactic potential*

At present, the constraints on the Galactic mass distribution, particularly in the vertical direction, are not very tight, so the range of plausible Galactic mass models remains large (Dehnen & Binney 1997). This means that the particular choice for the Galactic potential model could have biased the survivability of the models. To check this possibility, one of the robust dwarf galaxy models (K17-a) was simulated under the influence of three models for the Galactic potential. The mass fraction within 5 kpc of the center of the model at the end of the simulation is 77%, 86% and 56% (*cf.* Table 1), in, respectively, the Johnston *et al.* (1995) potential, the Evans & Jijina (1994) potential with  $q = 1$ , and the Evans & Jijina (1994) potential with  $q = 0.9$ . Thus the disruption rates, in these quite different, Galactic potentials are similar, which suggests that our results on the survivability of the Sagittarius dwarf are not very sensitive to the differences in *plausible* Galactic potential models. <sup>6</sup>

---

<sup>6</sup>The orbit in the flattened halo has a smaller periGalacticon passage, which leads to more rapid disruption.

### 5.1.2. *Evolutionary changes in the Galactic potential*

It has also been assumed that the Galactic potential is static. Clearly in the early stages of the formation of the Milky Way, the Galactic potential must have changed quite considerably. However, the thinness of the Galactic disk argues strongly (Tóth & Ostriker 1992) that the Galaxy did not suffer any major mergers since the formation of that component, more than 9.5 Gyr ago (Oswalt *et al.* 1996). Another way that the Galaxy may have grown is by the accretion of many small primordial clumps such as dwarf galaxies; as discussed further below, at least from spheroid stars in the Solar neighborhood halo (Unavane *et al.* 1996), one may rule out any substantial amount of accretion in this form onto the Milky Way. So though the assumption that the Galactic potential has not changed substantially over the last 12 Gyr is optimistic; it is probable that, for a large fraction of that time, it has remained approximately constant. If the potential gradients were substantially lower in the past, the tidal stresses on the Sagittarius dwarf would have been lower, and the simulations will have been biased to finding shorter survival times.

### 5.1.3. *The effect of the Magellanic Clouds*

We have assumed that the Milky Way provides the only significant external gravitational force field on the Sagittarius dwarf. However, it is conceivable that other members of the Galactic satellite system may play a rôle in its evolution. In particular, the Large and Small Magellanic Clouds are massive enough (respectively,  $6 \times 10^9 M_{\odot}$ , Meatheringham *et al.* 1988; and  $\sim 1.2 \times 10^9 M_{\odot}$ , Lin *et al.* 1995) to affect the orbit and the structure of the Sagittarius dwarf if they happen to pass sufficiently close to it. Even though the orbital plane of the Sagittarius dwarf spheroidal is almost perpendicular to that of the Magellanic Clouds, such a close encounter may indeed occur, given that the apoGalactic distance of  $\gtrsim 60$  kpc deduced above for the orbit of the Sagittarius dwarf is



approximately coincident with the present Galactocentric distance of the Magellanic clouds.

To investigate this possibility, we performed a simulation with three particles, representing the Sagittarius dwarf spheroidal, the LMC and the SMC. The kinematics of the Magellanic Clouds were taken from Kroupa & Bastian (1997), as determined from a mean of Hipparchos proper motions and earlier measurements. The Sagittarius dwarf was assumed to move on the orbit ‘a’, and to have a mass  $M = 10^9 M_{\odot}$ . The N-body code was used to integrate the motions of the three dwarf galaxies backwards in time, under the influence of the static potential of Johnston *et al.* (1995), with dynamical friction reversed. The forces were computed by direct summation, and a softening length of 1 kpc was adopted. With the above-stated parameters, the orbit of the Sagittarius dwarf is indeed altered by the Magellanic Clouds, but the effect is small, as can be seen from Figure 8. In Figure 9, the distance between the Sagittarius dwarf and each of the Magellanic Clouds is plotted as a function of time. Evidently, with the above parameters, the impact parameter never becomes smaller than 20 kpc.

To quantify the deviation on the orbit of the Sagittarius dwarf spheroidal due to the Magellanic Clouds, we performed 1000 simulations, each with a different, but equally likely, realization of the kinematic starting parameters of the Magellanic Clouds given the published errors (which we assume to be Gaussian). For each of these simulations, we computed the final (i.e. the primordial) radial period (defined as the time taken from apogalacticon to perigalacticon and back). The resulting distribution of radial periods in the ensemble of simulations is displayed in Figure 10; the mean of this distribution, at 1.09 Gyr, is very close to the unperturbed period of 1.08 Gyr, while the rms spread is 0.031 Gyr. The minimum and maximum periods found were 0.977 Gyr and 1.37 Gyr. In Figure 11 we show the distribution of minimum impact distances between the Sagittarius dwarf and the Magellanic Clouds. The probability of encounters with impact parameter

less than, say, 5 kpc, is 4.3%. Thus, it is very unlikely that the Magellanic Clouds alter significantly the orbital path of the Sagittarius dwarf, though there is a small chance that they may affect its internal dynamical evolution and its star-formation history. (The Sagittarius dwarf may similarly affect the Clouds). The effect of the extra gravitational perturbation will undoubtedly be to increase tidal disruption, and so diminish the lifetime of the Sagittarius dwarf. The fact that we neglected the Magellanic Clouds in the disruption simulations therefore poses no problem to our aim of placing a lower bound on the survival time of the Sagittarius dwarf.

#### 5.1.4. *Accretion onto the Sagittarius dwarf*

It was assumed that there has been no significant accretion onto the Sagittarius dwarf. Yet the Sagittarius dwarf spheroidal contains a mix of stellar populations, ranging from relatively old stars – many RR Lyrae stars are observed (Mateo *et al.* 1995, Alard 1996) and at least one of its globular clusters is as old as the oldest Galactic halo clusters (Richer *et al.* 1996, Chaboyer, Demarque and Sarajedini 1996) – to intermediate age stars – several Carbon stars have been identified (Ibata *et al.* 1994, 1995). It is unclear at present whether this complex star-formation history is the result of internal enrichment or accretion from beyond the dwarf. However, the accretion of a significant amount of matter onto the dwarf requires very special circumstances <sup>7</sup>, so it is more conservative to assume that only internal

---

<sup>7</sup>For instance, one can imagine an accretion scenario where clumps of gaseous material, driven out from the outer Galactic disk by SNe winds, attain velocities similar to the orbital velocity of the Sagittarius dwarf. As the Sagittarius dwarf passes close to such clumps, depending on relative velocities, some material within a Bondi–Hoyle radius could be accreted.

processing has produced the observed metal-rich stellar populations, and that the dwarf has only lost material.

#### *5.1.5. Effect of a collisional component*

We have also assumed that the dwarf was always entirely composed of collisionless particles. Clearly, a substantial gaseous component must have been present in the dwarf at each stage of star-formation. However, we can expect that most such material would be stripped from the dwarf during its collisional encounters with the Galactic disk. If there was no significant accretion, the periodic removal of gas from the Sagittarius dwarf would have the effect of lowering the total mass, thereby reducing its survival time. By not including this effect, we have under-estimated the disruption rate, which is not a worry in terms of our aim of determining a lower bound to the survival time.

## **5.2. Survival of primordial galaxy fragments**

One of the most significant consequences of the failure of the mass-traces-light models to reproduce the observations is that the merging fragments that made the Galaxy probably had a radially increasing mass to light ratio, so that the stars were more centrally concentrated and the dark matter more extended. Detailed numerical simulations are required to explore this question further, but one may expect such a structure to initially lose almost exclusively dark matter, with stars being lost only in the last stages of disruption. If dynamical friction causes significant orbital decay of the merging clumps, the luminous matter would be deposited more centrally than the dark matter in the global potential well, naturally giving rise to a radially increasing mass to light ratio in the halos of large galaxies.

We have shown that, even in the absence of a dark matter component, some dwarf galaxy models (those a small initial half-mass radius) may survive almost intact in the Galactic halo, even on such short period orbits as that deduced for the Sagittarius dwarf. Furthermore, the range of allowable initial structural parameters of the models is quite large. One may deduce from these facts that a significant fraction of the primordial population of dwarf galaxies with initial half mass radius  $\sim 1/3$  of that of the Sagittarius dwarf managed to survive until the present day; this holds as long as the orbits of the population of proto-dwarf galaxies were not significantly more biased towards radial orbits, where smaller perigee distances give rise to faster disruption. The observed paucity of such galaxies in the Milky Way halo therefore provides strong evidence that the primordial population was not numerous. This conclusion is consistent with the findings of Unavane *et al.* (1996), who, from counts of Solar neighborhood spheroid stars blue-ward of  $B - V = 0.4$ , put a limit on the merging rate into the Galactic halo of 40 Carina-like dSph, or 5 Fornax-sized dSph in the last 10 Gyr.

However, some cautionary remarks on the Unavane *et al.* (1996) technique should be made. In all our simulations, the material disrupted from the models is confined to long streams that persist for at least 12 Gyr. The mass density along the streams is inversely related to the orbital velocity, so most of the disrupted mass lies at large Galactocentric radii. Also, a negligible fraction of the disrupted particles attain orbits with significantly lower perigee distance than the parent satellite. For these reasons, one may expect disrupted dwarf galaxies to contribute a negligible fraction of their mass to the Solar neighborhood. Only stars disrupted from those dwarf galaxies that had small periGalactic distances, but long enough orbital periods not to have been destroyed at the earliest epochs, will be seen near the Sun; furthermore, the kinematics of such stars will likely be quite different from that of the spheroid.

Recently, Kroupa (1997) has argued that the high mass to light ratios inferred for dSph galaxies are incorrect, because the measured high velocity dispersion arises from viewing tidal debris along a disruption orbit that is approximately parallel to the line of sight. If so, the present day dSph are only small remnants containing  $\sim 1\%$  of the original mass of these galaxies. Though this may a feasible explanation for the velocity dispersion of some of the small dSphs, this suggestion cannot possibly hold for the Sagittarius dwarf, as the constraints on disrupted material from are quite strong. If the Sagittarius dwarf at the present day contained only  $\sim 1\%$  of the original galaxy, we would expect to see  $\sim 400$  globular clusters on the great circle of its orbit. This is clearly inconsistent with observations.

### 5.3. Predictions of the models

All of the simulations give rise to streams of tidally disrupted material that follow the orbital path of the remnant quite closely. The disrupted fraction always exceeded 15%, though we stress that this is simply indicative, since we have not managed to make any model fit the available data. So we may expect to find a sizeable fraction of the stellar component of the Sagittarius dwarf spheroidal, including perhaps one or more globular clusters, stretching along a ring around the sky. An interesting feature of the streams is that they become narrow near perigee and broad at apogee. It will be very fruitful to detect such material, as its kinematics could provide a very sensitive test of the Galactic potential gradients; we will discuss this further in a subsequent contribution.

As discussed in IWGIS, the mass range of Sagittarius dwarf galaxy models that contain dark matter, suggest that the Milky Way itself is significantly affected by the passage of the Sagittarius dwarf; certainly the tidal forces on the Milky Way due to the Sagittarius dwarf are substantially larger than those due to the Large Magellanic cloud, which has

previously been invoked as a possible perturber of the H I disk (Weinberg 1995). Thus, the star-formation history of the Galaxy may have been influenced by this dwarf. To quantify the picture, it will be necessary to determine the mass of the dwarf as accurately as possible. Such a study is possible by combining an accurate photometric profile (which has not as yet been obtained) with the extant velocity dispersion profile. This information determines both the present-day dark matter profile and the present total mass. Detailed N-body simulations, with a stellar component embedded in the dark matter, will then have to be performed to check the robustness of the models and whether the end-point structure can be made to be consistent with observations. This gives an opportunity to determine the distribution of dark matter in a dwarf galaxy.

## 6. Conclusions

Comparison of the observed velocity profile to the simulations presented above indicates that the Sagittarius dwarf has a short period orbit, with radial period  $T \sim 0.7$  Gyr. It is found that any reasonable model of the internal structure of the dwarf galaxy, where light traces mass and where  $M/L \lesssim 10$ , either does not survive the tidal interaction with the Milky Way, or has a minor axis half-mass radius that is inconsistent with observations. Thus, it is not possible to understand the present existence of the Sagittarius dwarf spheroidal if most of its mass is in the form of stars. However, this problem may be solved if Sagittarius, and by implication, other dwarf spheroidal galaxies, have a radially increasing mass to light ratio, as suggested by IWGIS. This analysis supports the mass to light ratio determination of IWGIS, who found  $M/L_{\text{global}} \sim 100$ .

This conclusion should still hold if there is internal rotation in the dwarf. Nor should the conclusion be affected significantly by the choice of Galactic potential model. The perturbative effect of the Magellanic Clouds was considered; given current estimates of their

kinematics, there is a negligible chance that they could have altered sufficiently the orbit of the Sagittarius dwarf to account for the short period deduced above.

Further numerical work is required to construct a fully self-consistent model in which both the stellar and dark matter components are present and can reproduce the observations.

We are very grateful to Derek Richardson for kindly letting us use of his `box_tree` code and related plotting routines, and especially for many illuminating email conversations. We also cordially thank G. Fahlman, K. Menon, H. Richer, D. Scott and G. Walker for generous loan of their computer resources. RAI expresses gratitude to the Killam Foundation (Canada) and to the Fullam Award for support.

## REFERENCES

- Alard, C. 1996, ApJ 458, L17
- Bender, R., Nieto, J. 1990, A&A 239, 97
- Binney, J. 1978, MNRAS 183, 501
- Binney, J. & Tremaine, S., 1987 ‘Galactic Dynamics’ (Princeton University Press, Princeton)
- Chaboyer, B., Demarque, P. & Sarajedini, A. 1996, ApJ 459, 558
- Dekel, A. & Silk, J. 1986, ApJ 303, 39
- Dehnen, W. & Binney, J. 1997, astro-ph/9612059
- Englmaier, P., 1997, Ph.D. Thesis, Basel
- Evans, N. & Jijina, J. 1994, MNRAS 267, L21
- Faber, S. & Lin, D. 1983, ApJ 266, L17
- Fahlman, G., Mandushev, G., Richer, H., Thompson, I., & Sivaramakrishnan, A. 1996, ApJ 459L, 65
- Hernquist, L. 1990, ApJ 356, 359
- Ibata, R., Gilmore, G., & Irwin, M. 1994, Nature 370, 194.
- Ibata, R., Gilmore, G., & Irwin, M. 1995, MNRAS 277, 781
- Ibata, R., Wyse, R., Gilmore, G., Irwin, M. & Suntzeff, N., 1997, AJ 113, 634
- Irwin, M. & Hatzidimitriou, D., 1995, MNRAS 277, 1354
- Irwin, M., Ibata, R., Gilmore, G., Suntzeff, N. & Wyse, R. 1996, in: ‘Formation of the Galactic Halo’, ed A. Sarajedini, A.S.P., San Francisco
- Johnston, K. V., Spergel, D. N., & Hernquist, L. 1995, ApJ 451, 598
- Johnstone, D. 1993, AJ 105, 155



- King, I. 1966, AJ 71, 64
- Kroupa, P., & Bastian, U. 1997, *New Astronomy* 2, 77
- Kroupa, P. 1997, *New Astronomy* 2, 139
- Lin, D., Jones, B. & Klemola, A. 1995, ApJ 439, 652
- Meatheringham, S., Dopita, M., Ford, H. & Webster, B. 1988, ApJ 327, 651
- Mateo M., Udalski A., Szymanski M., Kaluzny J., Kubiak M. & Kreminski W. 1995a, AJ 109, 588
- Mateo, M., Mirabal, N., Udalski, A., Szymanski, M., Kaluzny, J., Kubiak, M., Kreminski, W. & Stanek, K. 1996, ApJ 458, L13
- Miyamoto, M. & Nagai, R. 1975, PASJ 27, 533
- Oh, K.S., Lin, D.N. & Aarseth, S.J. 1995, ApJ 442, 142
- Oswalt, T., Smith, J., Wood, M. & Hintzen, P. 1996, *Nature* 382, 692
- Piatek, S. & Pryor, C. 1995, AJ 109, 1071
- Pryor, C. & Meylan, G. 1993, in: ‘Structure and Dynamics of Globular Clusters’, eds S. Djorgovski and G. Meylan, A.S.P., San Francisco
- Richardson, D. 1993, Ph.D. Thesis, Cambridge
- Richer, H., Harris, W., Fahlman, G., Bell, R., Bond, H., Hesser, J., Holland, S., Pryor, C., Stetson, P., Vandenberg, D. & van den Bergh, S. 1996, ApJ 463, 602
- Sandage, A., 1965, in ‘The Structure and Evolution of Galaxies’, ed. H. Bondi (New York, Interscience), p83
- Spitzer, L. 1987, ‘Dynamical Evolution of Globular Clusters’, (Princeton University Press, Princeton)
- Tóth, G. & Ostriker, J., 1992, ApJ 389, 5

Unavane, M., Wyse, R. & Gilmore, G. 1996, MNRAS 278, 727

Velasquez, H. & White, S. 1995, MNRAS 275, L23

Weinberg, D. 1995, ApJ 455, L31

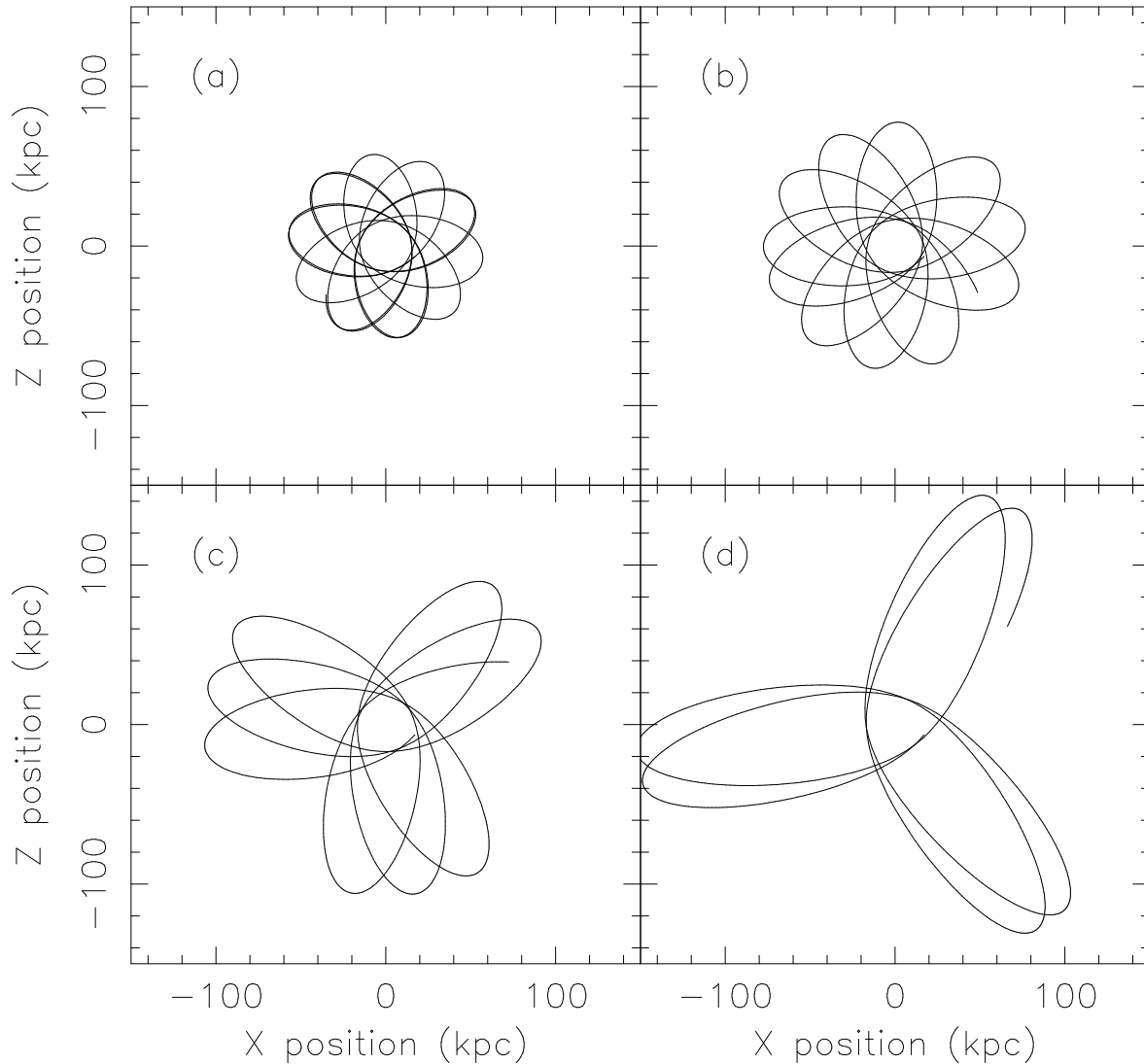


Fig. 1.— These diagrams show the  $x$ - $z$  structure of the orbit of a test particle (i.e., negligible dynamical friction) integrated backwards in time for 12 Gyr under the influence of the Galactic potential detailed in the text. The orbit in panel ‘a’ is derived from the best fit to the kinematic and distance observations. This orbit has a total velocity of  $|v_{com}| = 332 \text{ km s}^{-1}$  at the present position of the Sagittarius dwarf. However, for reasons detailed in the text, we also explore the behavior of the dwarf galaxy structural models on the longer period orbits shown in panels ‘b’, ‘c’ and ‘d’, which have  $|v_{com}| = 362 \text{ km s}^{-1}$ ,  $392 \text{ km s}^{-1}$  and  $422 \text{ km s}^{-1}$ , respectively.

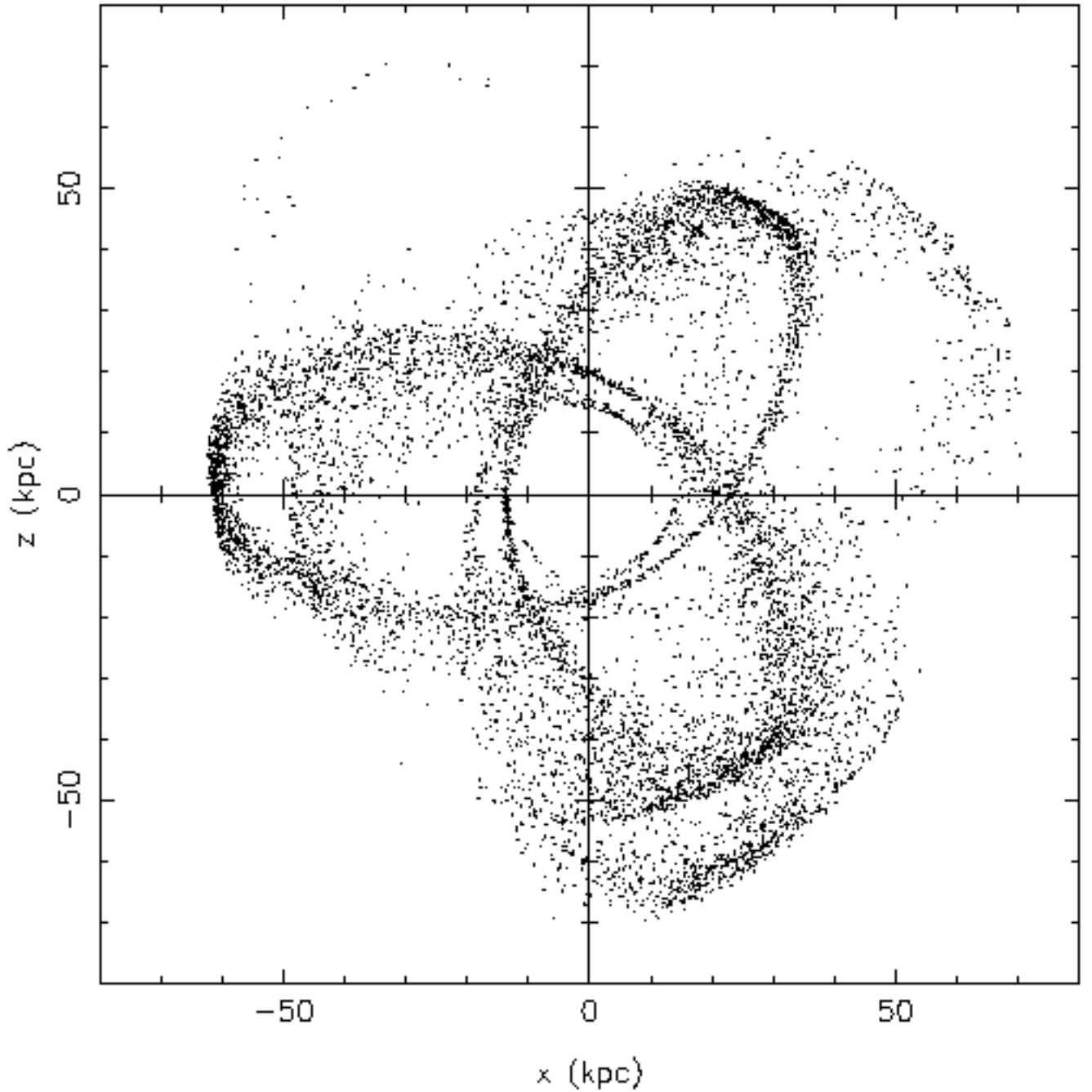


Fig. 2.— The  $x$ - $z$  plane structure of the remnant of the dwarf galaxy model K1-a, whose initial structure fits best the present-day observations of the Sagittarius dwarf, is shown at the end-point of the integration. All traces of a central concentration have vanished.

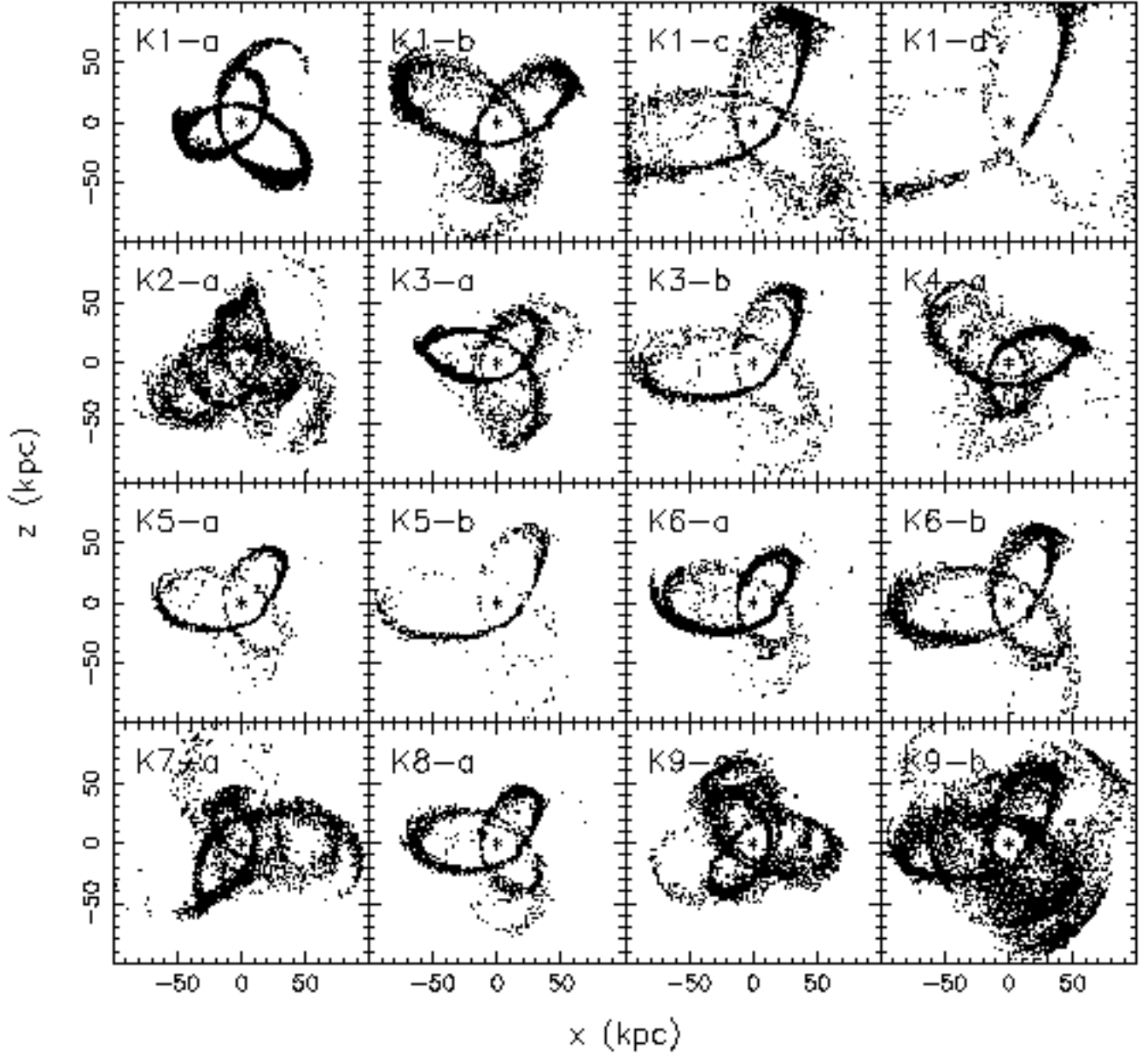


Fig. 3.— The structure of all the King model simulations (except the two models simulated with the Galactic potential of Evans & Jijina 1994) is displayed at the simulation time  $T_{ok}$ . Each panel is marked with the model identification label, as given in column (1) of Table 1.

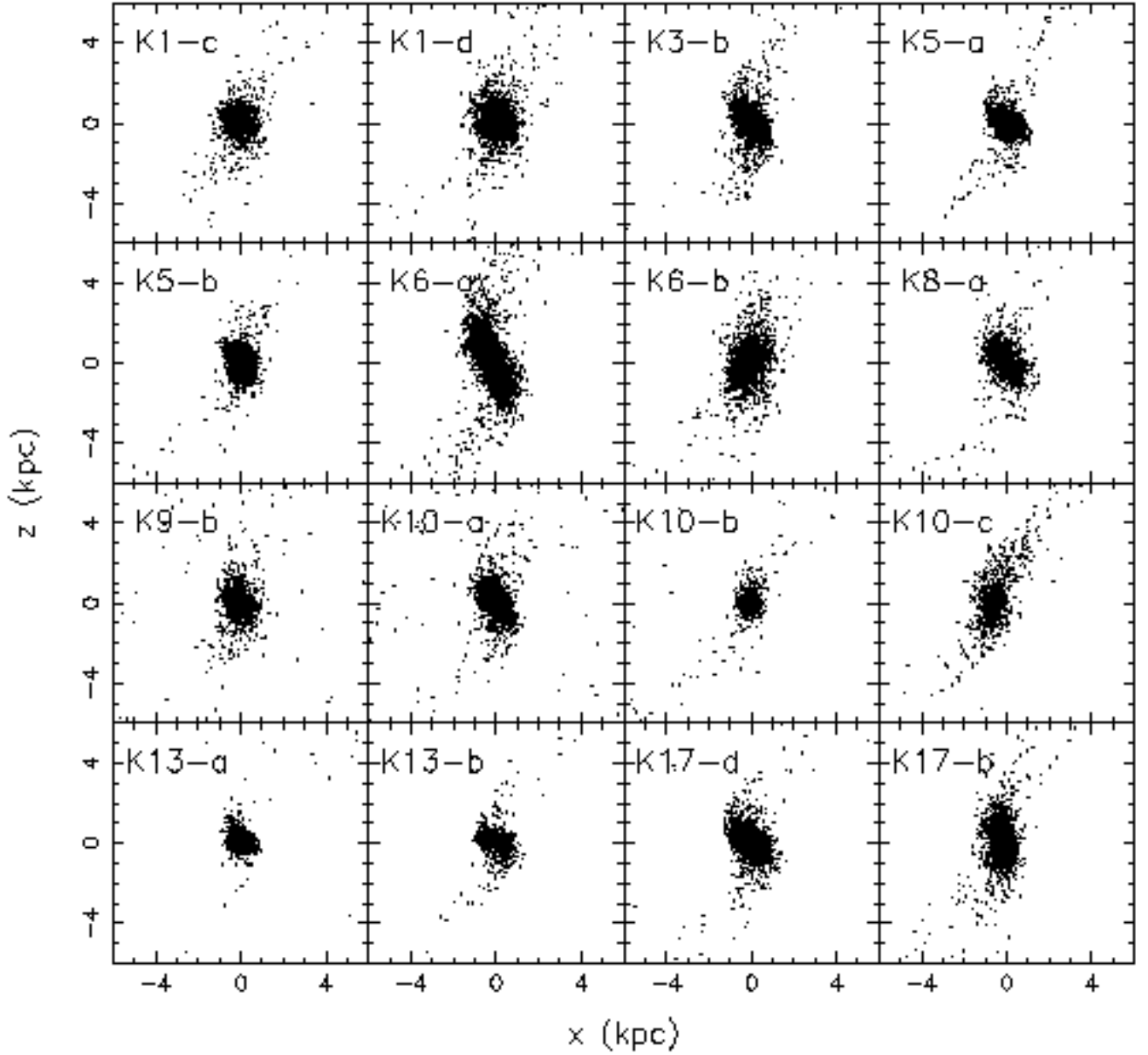


Fig. 4.— A close-up picture of the end-point structure of all the models in Figure 3 that managed to retain a central concentration until the end of the simulation.

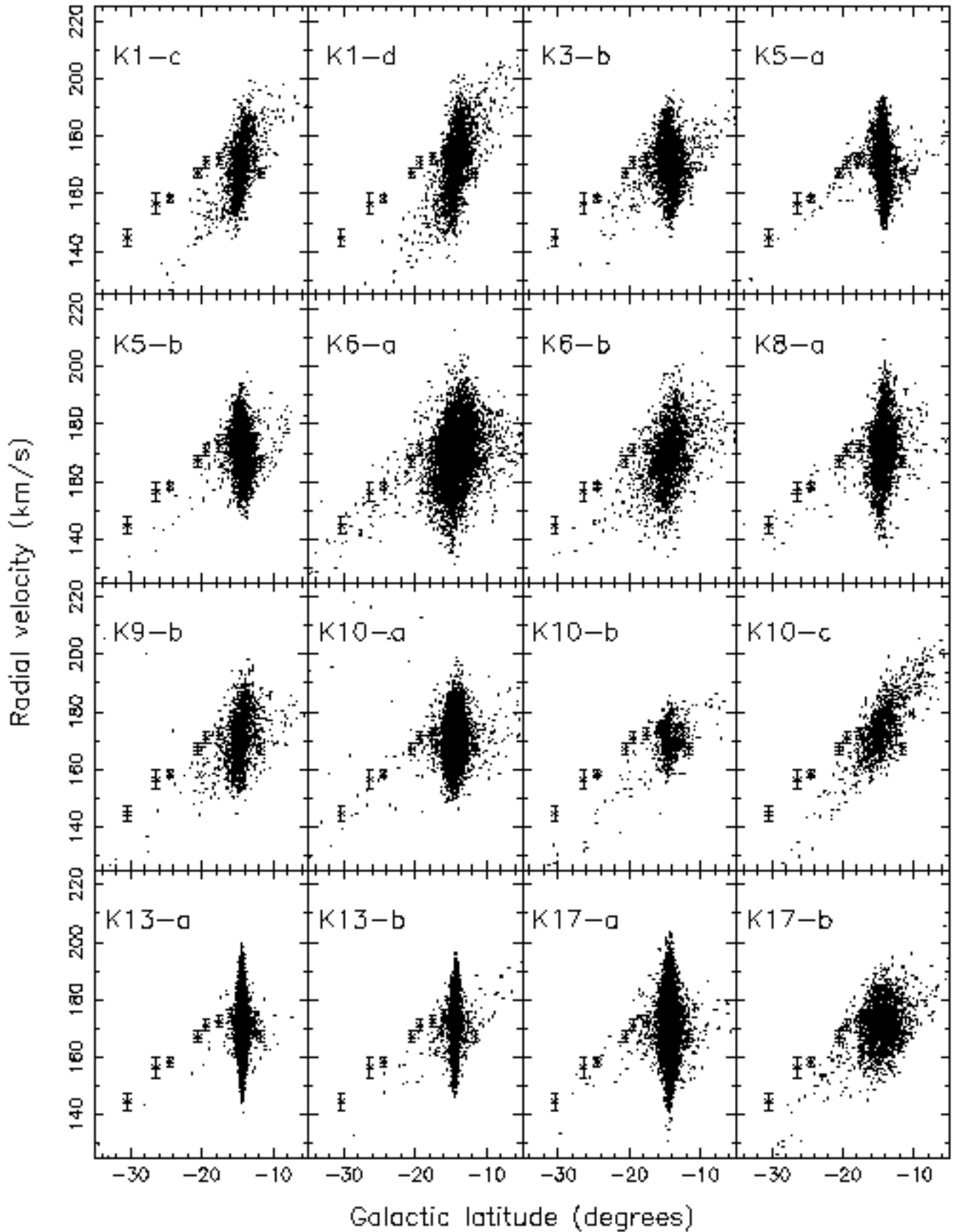


Fig. 5. The observed radial velocity gradient is compared to the models displayed in

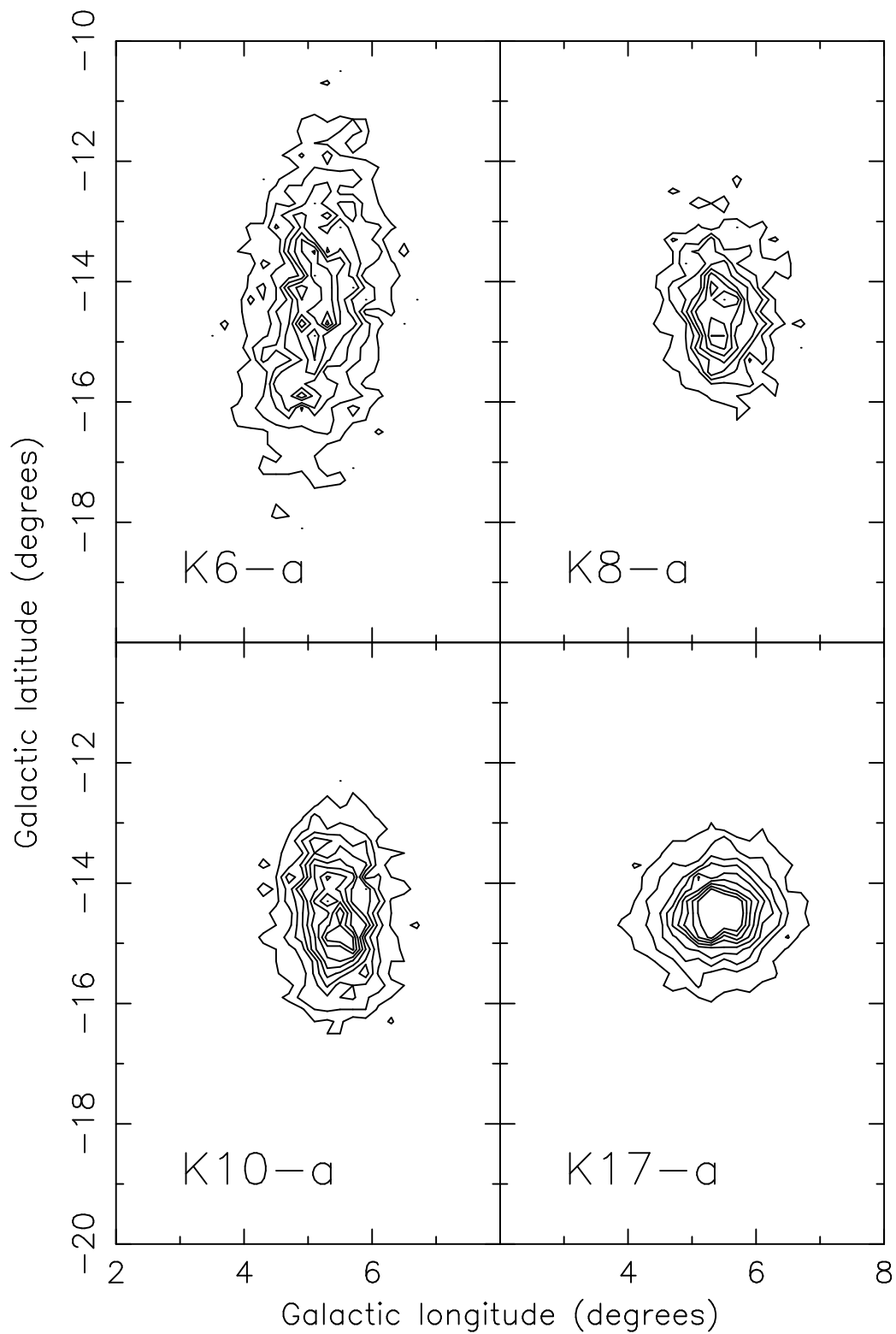


Fig. 6.— The final surface number density of particles from four robust King models that give a good representation of the kinematic observations, are displayed. However, all four models have a minor axis half-mass radius  $R_{HB} < 0.21$  kpc, inconsistent with the observed value of  $R_{HB} \sim 0.55$  kpc.



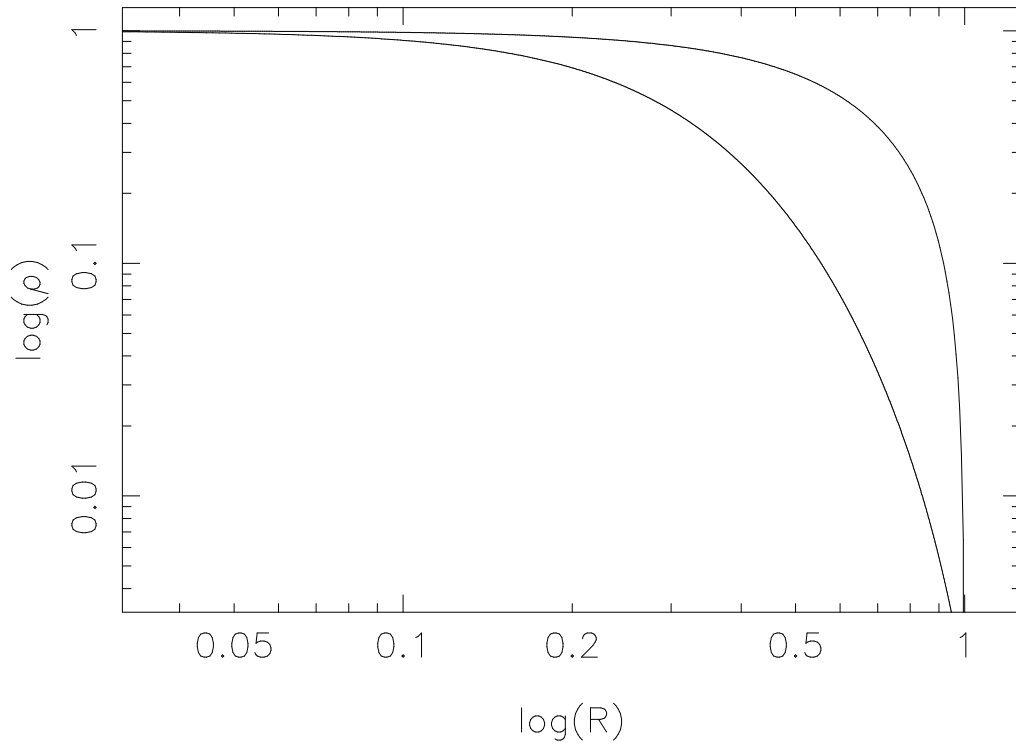


Fig. 7.— The density profile of the Gaussian model described in the text (top curve) is compared to the very low concentration King model K17 (bottom curve).

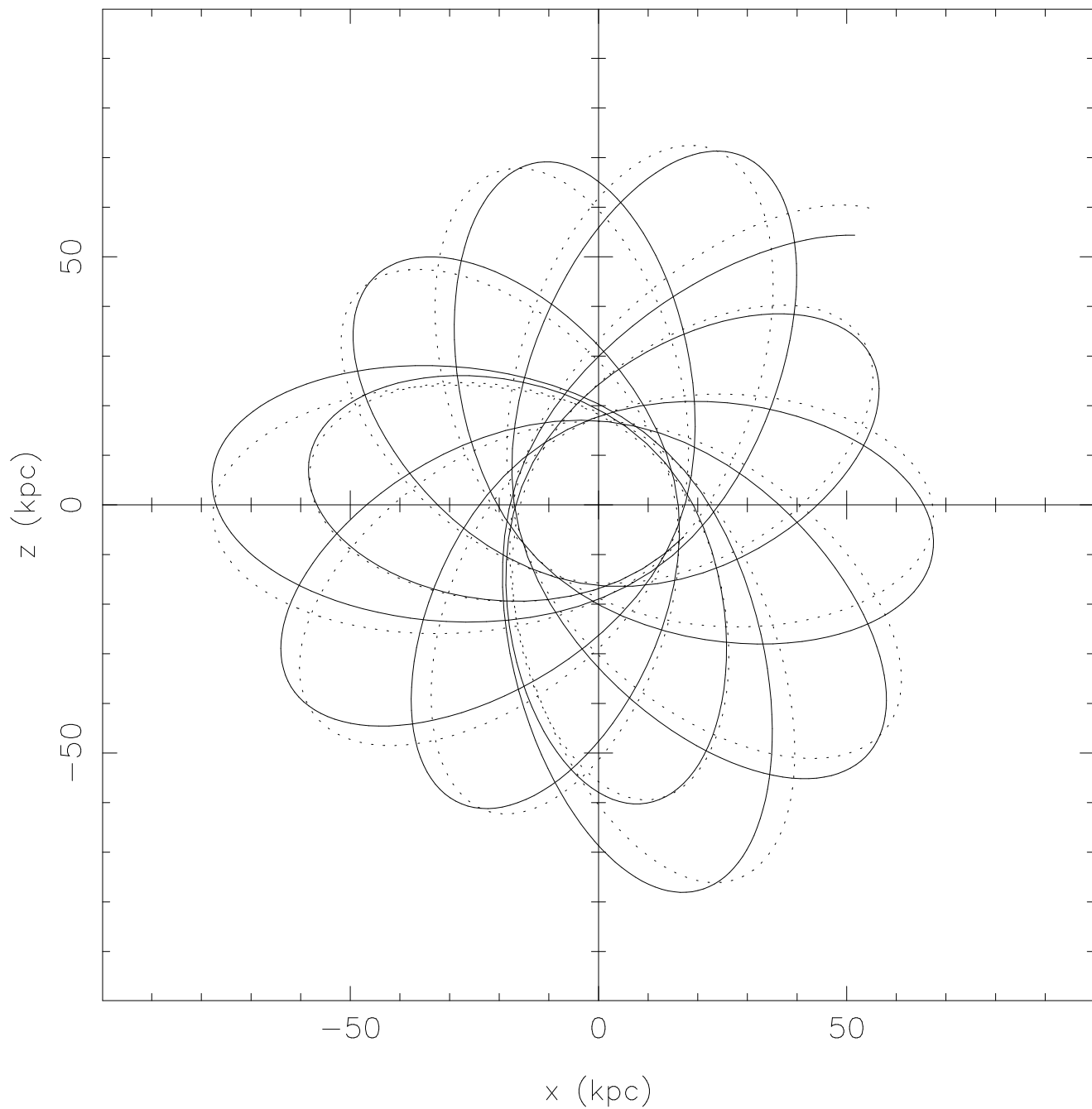


Fig. 8.— The solid line shows the path, in the  $x$ - $z$  plane of the Galaxy, of a  $M = 10^9 M_{\odot}$  point-like particle that moves purely under the influence of the assumed Galactic potential for 12 Gyr. The initial velocity parameters of the particle correspond to those of orbit ‘a’. The dotted line shows the perturbed path taken by the same particle when point masses, representing the Small and Large Magellanic Clouds, are included into the integration.

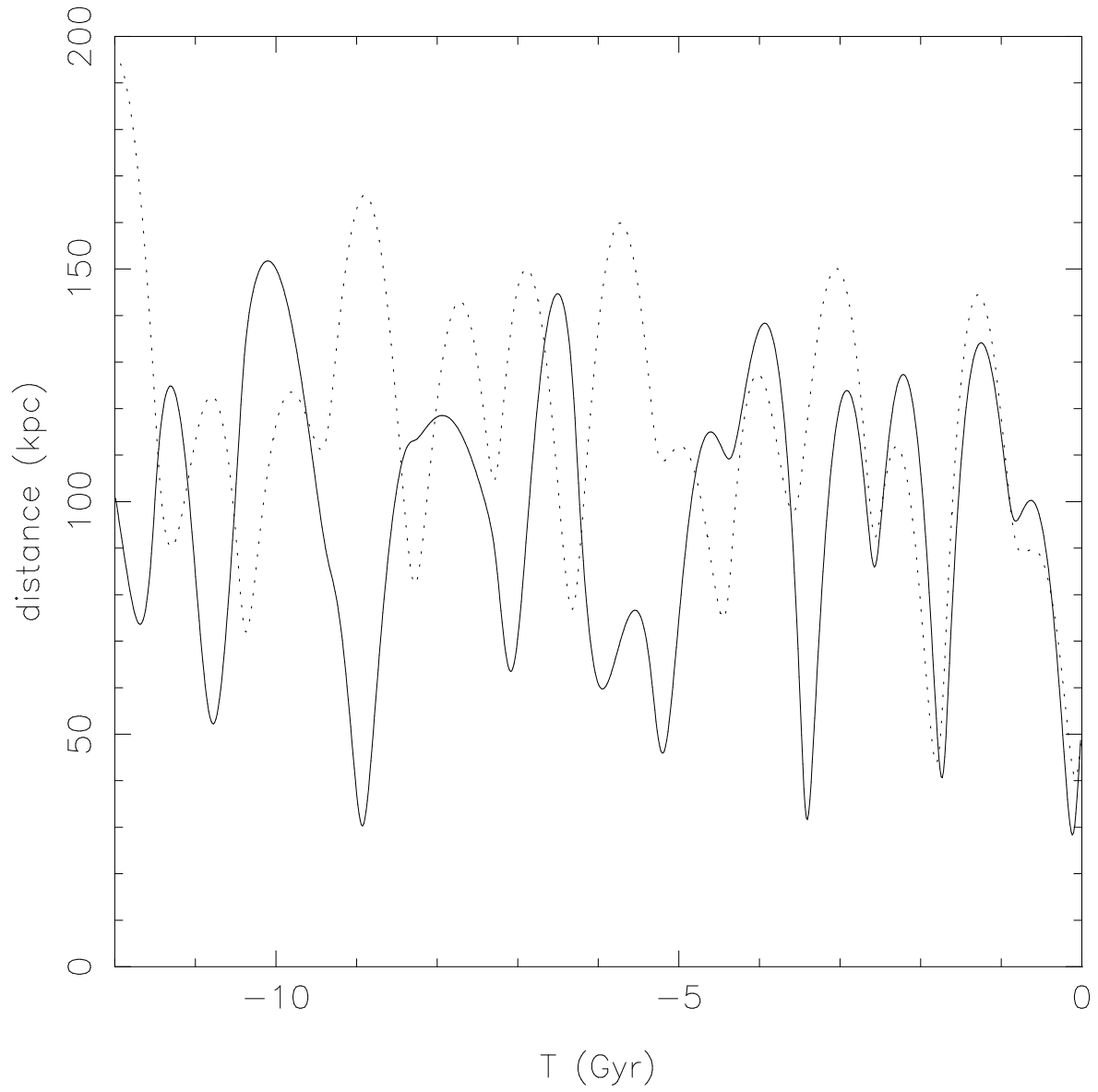


Fig. 9.— The distance between the Sagittarius dwarf and, respectively, the LMC (solid line) and the SMC (dotted line) in the simulation of Figure 8 are displayed as a function of time. The time  $T = 0$  corresponds to the present day.

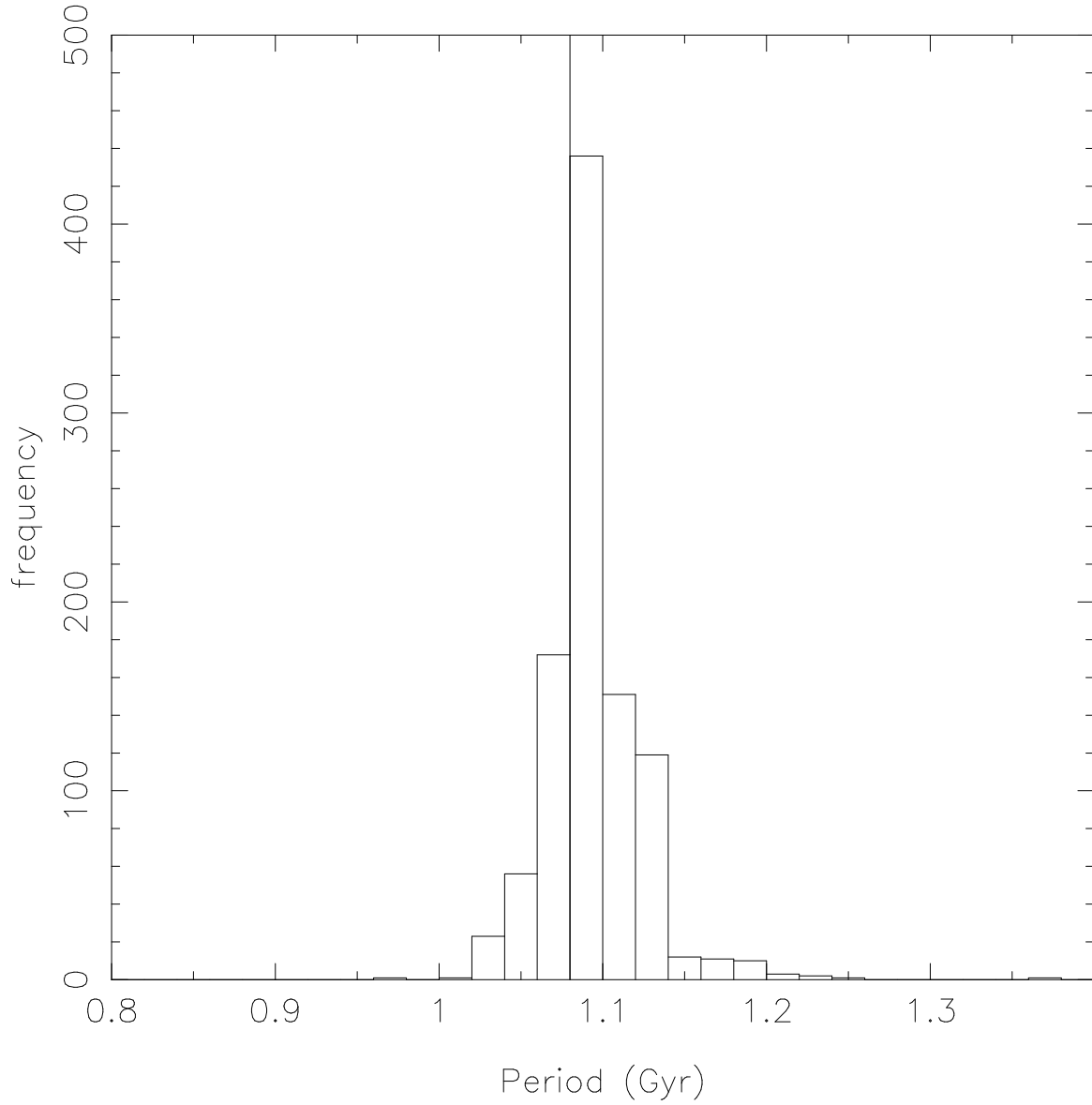


Fig. 10.— The probability distribution of initial (i.e. primordial) radial periods of the Sagittarius dwarf in the presence of the Magellanic Clouds. Clearly, the period of the Sagittarius dwarf is not significantly altered by these perturbers.

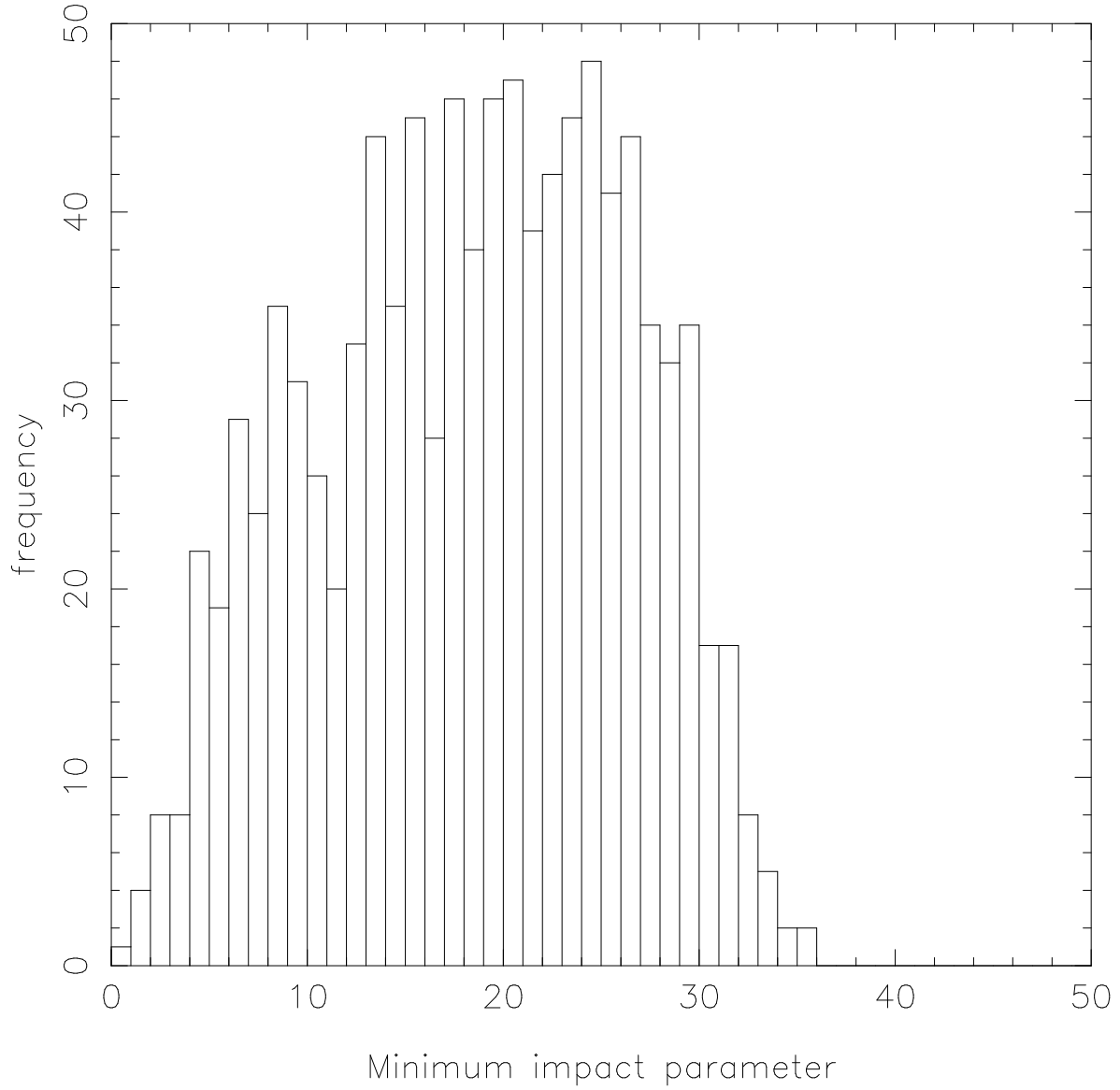


Fig. 11.— The distribution of minimum impact parameters between the Sagittarius dwarf and the Magellanic Clouds. The chance of a close encounter having taken place in the past appears to be significant, but not large.

TABLE 1  
KING MODEL SIMULATIONS

model	$\left(\frac{\Psi}{\sigma^2}\right)_0$	$\rho_0$ ( $\frac{M_\odot}{pc^3}$ )	$\sigma$ ( $\frac{km}{s}$ )	$\sqrt{v_x^2}$ ( $\frac{km}{s}$ )	$R_{HB}$ (kpc)	$R_T$ (kpc)	$M$ ( $10^9 M_\odot$ )	$N$ ( $10^3$ )	$\log(T_{ev})$ (yr)	$T_{dis}$ (Gyr)	$T_{ok}$ (Gyr)	$\left(\sqrt{v_r^2}\right)_{T_{ok}}$ ( $\frac{km}{s}$ )	$R_{HB}(T_{ok})$ (kpc)
K1-a	2.0	0.1	20.0	11.3	0.51	2.6	0.15	8	11.4	5.4	5.0	8.0	0.36
K1-b								4	11.2	8.6	8.9	7.2	0.28
K1-c								4		(26%)	(36%)	9.2	0.36
K1-d								4		(44%)	(59%)	10.4	0.22
K2-a			40.0	18.9	1.0	5.2	1.2	4		7.1	6.4	14.8	0.10
K3-a		0.5	23.0	10.9	0.26	1.3	0.10	4	10.9	11.1	11.4	10.0	0.22
K3-b								4		(72%)	(85%)	9.8	0.19
K4-a			40.0	18.9	0.45	2.3	0.55	4	10.8	9.6	9.6	13.7	0.30
K5-a		2.0	25.0	11.8	0.14	0.7	0.07	4	10.5	(70%)	(78%)	9.3	0.14
K5-b								4		(78%)	(86%)	7.5	0.16
K6-a			40.0	18.9	0.27	1.2	0.27	8	11.0	(40%)	(58%)	12.3	0.18
K6-b								4	10.8	(33%)	(44%)	10.6	0.27
K7-a			80.0	37.9	0.45	2.3	2.2	4	10.5	8.6	7.8	23.5	0.23
K8-a		5.0	40.0	18.9	0.14	0.7	0.17	4	10.3	(51%)	(60%)	12.5	0.15
K9-a	6.0	0.2	16.5	11.3	0.44	8.5	0.36	4	10.4	10.4	7.8	8.9	0.19
K9-b								8	10.6	(12%)	(18%)	8.7	0.19
K10-a		1.0	16.5	11.1	0.20	3.8	0.16	8	10.3	(31%)	(41%)	10.3	0.20
K10-b								4	10.1	(40%)	(52%)	9.6	0.16
K10-c								4	10.1	(25%)	(12%)	9.0	0.19
K11-a		3.0	20.0	13.2	0.13	2.7	0.16	4	9.7	10.4	10.7	10.1	0.13
K12-a			40.0	26.5	0.28	5.4	1.3	4	9.8	7.0	6.4	17.8	0.25
K13-a		10.0	16.5	11.0	0.07	1.3	0.05	8	9.9	(83%)	(84%)	11.7	0.08
K13-b								4	9.7	(68%)	(73%)	9.5	0.10
K14-a			40.0	26.5	0.15	2.9	0.73	4	9.5	9.0	8.1	12.0	0.20
K15-a			80.0	53.0	0.30	5.7	5.9	4	9.5	6.2	5.6	24.2	0.15
K16-a	0.5	0.1	45.0	11.2	0.59	2.4	0.22	4	12.4	5.5	5.8	7.6	0.15
K16-b								4		9.8	10.1	8.2	0.23
K17-a		0.5	50.0	12.1	0.29	1.2	0.14	8	12.3	(72%)	(77%)	12.8	0.21
K17-a <sup>†</sup>								8		(76%)	(85%)	12.2	0.22
K17-a <sup>††</sup>								8		(46%)	(56%)	11.0	0.20
K17-b								4	12.0	(27%)	(50%)	7.6	0.09
K18-a			100.0	26.7	0.59	2.4	1.08	4	12.1	8.7	8.7	22.5	0.22
K19-a		2.0	100.0	25.0	0.29	1.2	0.54	4	11.8	10.2	9.3	11.8	0.27
K20-a		5.0	100.0	25.0	0.19	0.8	0.34	4	11.6	9.5	8.8	11.1	0.20

<sup>†</sup>Evans & Jijina (1994) potential, with halo flattening  $q = 1.0$ .

<sup>††</sup>Evans & Jijina (1994) potential, with halo flattening  $q = 0.9$ .